Surface Science 198 (1988) 331–359
North-Holland, Amsterdam

ON THE ELECTRONIC STRUCTURE OF THE COADSORBATE SYSTEM CO + O (2 × 1)/Pd(111): A PRECURSOR FOR CO_2 FORMATION *

G. ODÖRFER, E.W. PLUMMER **, H.-J. FREUND

Lehrstuhl für Physikalische Chemie I, Ruhr-Universität Bochum, 4630 Bochum 1, Fed. Rep. of Germany

H. KUHLENBECK and M. NEUMANN

Fachbereich Physik, Universität Osnabrück, Barbarastrasse 7, 4500 Osnabrück, Fed. Rep. of Germany

Received 23 November 1987; accepted for publication 25 January 1988

We report results of an angle resolved photoelectron spectroscopy (ARUPS) study using synchrotron radiation from the BESSY storage ring of the CO + O (2 × 1)/Pd(111) coadsorbate system in comparison with the CO($\sqrt{3} \times \sqrt{3}$)R30°/Pd(111) adsorbate. The band structures of the CO induced $5\sigma/1\pi$ and 4σ levels for both structures are observed and favourably compared with the proposed structure models as well as tight-binding model calculations. Light polarization dependent measurements as well as the angle dependence of the 4σ shape resonance indicate that the CO molecular axis in the pure CO adsorbate is perpendicular to the Pd(111) surface, while it appears slightly (< 10°) inclined with respect to the surface normal in the coadsorbate. We show by comparison with other pure CO adsorbates using the measured E versus $k_{\parallel}$ dispersions that the 4σ wave function in the coadsorbate is very similar to the pure adsorbate. It is shown that this is different with respect to other, namely CO + K, coadsorbates.

1. Introduction

Coadsorption and mutual interaction between adsorbed species form the basis for understanding the microscopic steps of surface reactions. CO oxidation more than the reverse reaction, i.e. CO_2 dissociation, has been a model reaction for which the adsorption of reaction educts and the interaction of reaction products as well as the nature of reaction precursor species have been studied [1–17]. Two observations are mentioned: Ertl and coworkers [1,10] showed via molecular beam studies that CO oxidation proceeds according to a

* Work started at: Institut für Physikalische und Theoretische Chemie, Universität Erlangen-Nürnberg, Egerlandstrasse 3, 8520 Erlangen, Fed. Rep. of Germany.

** Permanent address: Department of Physics, University of Pennsylvania, Philadelphia, PA 19104, USA.

Langmuir–Hinshelwood mechanism where both reactants are adsorbed on the surface. A bent O · · · CO precursor for the formation of CO_2, with the nascent O · · · C bond being coordinated in a local C_s symmetry to the metal surface, was postulated [11]. Adsorbed molecular CO_2 has not been observed. Recently, however, a precursor for CO_2 dissociation has been identified and characterized using angle resolved photoelectron spectroscopy (ARUPS) [18–20], and high resolution electron energy loss spectroscopy (HREELS) [18], as well as near edge X-ray absorption fine structure measurements (NEXAFS) [21] on Ni(110) to be a bent, anionic CO_2 species which is – most likely – coordinated with its oxygen atoms to the metal surface in a local C_{2v} symmetry.

In order to understand the electronic structure of CO interacting with O in an effort to try to isolate the factors that influence the interactions in the CO–O coadsorbate, and relate the results with those on CO_2 dissociation, we have studied the CO + O (2 × 1)/Pd(111) system. There have been rather detailed accounts of the surface interactions of oxygen and CO on Pd(111)

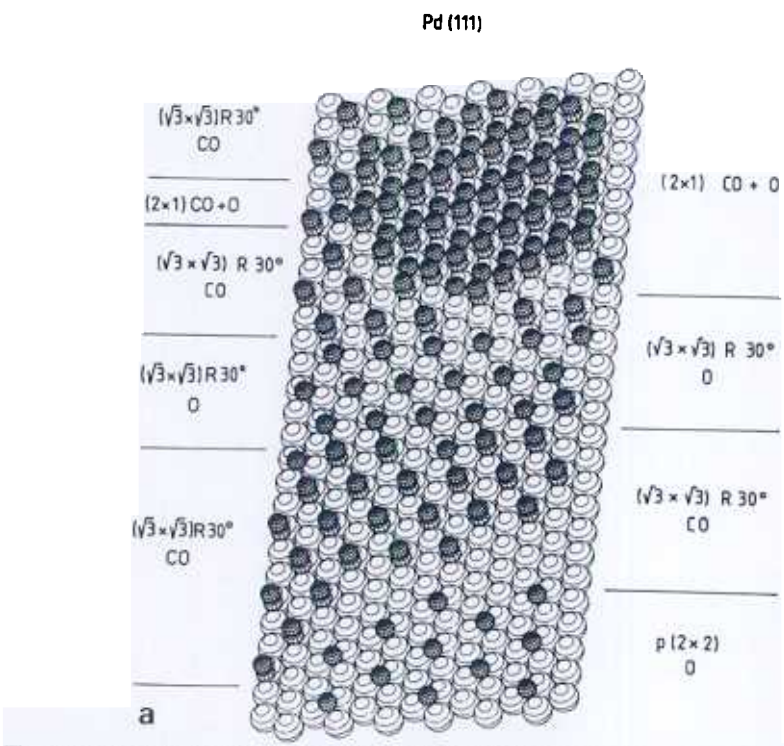

Fig. 1a. Schematic three-dimensional representation of the structural transformations taking place when an oxygen precovered surface is exposed to CO. For the CO + O (2×1) structure only one domain is shown.

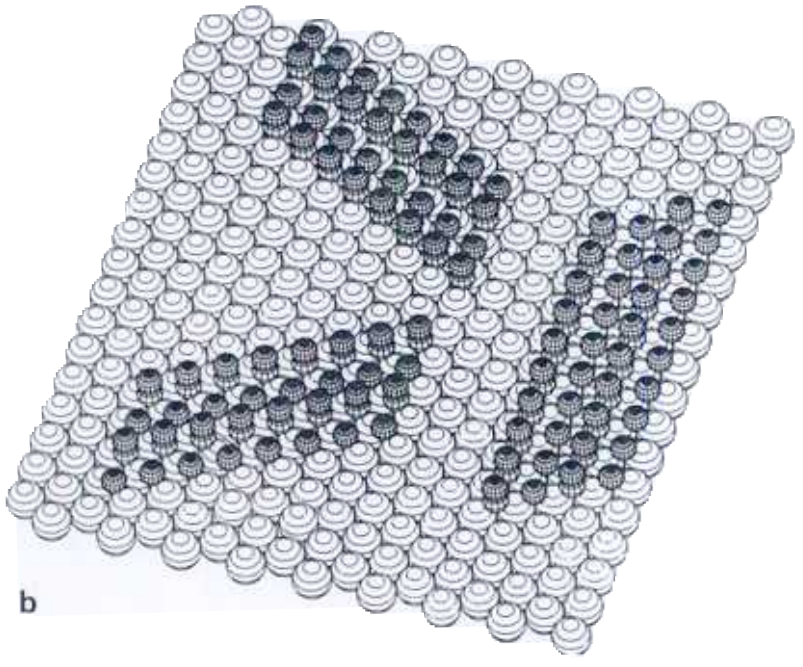

Fig. 1b. Schematic three-dimensional representation of the orientations of the three domains of a CO + O (2×1)/Pd(111) structure.

using thermal desorption spectroscopy (TDS) [2], low energy electron diffraction (LEED) [2,9,14], and ultraviolet photoelectron spectroscopy (UPS) [9,14].

Briefly, the adsorption behaviour is asymmetric which means that preadsorbed CO inhibits oxygen adsorption whereas the reverse is not the case [1]. The situation is schematically shown in fig. 1a [2,9]. A Pd(111) surface saturated with oxygen exhibits a p(2 × 2) LEED pattern. Upon exposure to CO the oxygen p(2 × 2) domains are compressed into domains with a ($\sqrt{3}$ × $\sqrt{3}$)R30° LEED pattern by coadsorbed CO which itself gives rise to the same ($\sqrt{3}$ × $\sqrt{3}$)R30° LEED pattern (the same monolayer structure that is formed upon pure CO adsorption). Further exposure of this domain structure to CO leads to the formation of regions on the surface that give rise to a (2 × 1) LEED pattern, and which are assigned to a mixed O–CO phase with alternating CO and oxygen rows [2,9,14]. Fig. 1a only shows one out of three domains of the (2 × 1) structure. The three domains and their relative orientations are depicted in fig. 1b. Note, however, that the CO + O (2 × 1) structure has to our knowledge not been analysed via an LEED I/V study. Therefore, the adsorption sites (twofold bridges) proposed in fig. 1 must be considered as tentative [22]. The (2 × 1) structure is always accompanied by ($\sqrt{3}$ × $\sqrt{3}$)-R30°

domains of adsorbed CO. The CO + O (2 × 1) coadsorbate releases CO_2 upon raising the temperature with high yield [1,2]. Extremely sharp angular distributions observed in TDS with collimation of the desorbing CO_2 molecules along the surface normal for the (2 × 1) structure [2] support the idea of CO and O being adsorbed in adjacent sites.

It has been pointed out by Engel and Ertl [1] that it might be the compression and "interdiffusion" of oxygen and CO "domains" which activates the adsorbate system and finally leads to the formation of CO_2. The mixed CO + O (2 × 1) coadsorbate configuration exhibits the highest reactivity manifested by the tendency to form CO_2 well below room temperature. Even though this highly reactive configuration will presumably not be reached under steady state reaction conditions it is well suited to study CO–oxygen interaction because the number of CO–O pairs in intimate contact is highest. Obviously, one would expect a variation in the electronic properties of both O and CO when the two components are in close proximity. Indeed, Conrad et al. [9,14] have found a shift in the valence ionizations of CO in the CO + O (2 × 1) coadsorbate phase as compared to pure CO using angle integrated photoelectron spectroscopy. With ARUPS we are now in a position to investigate the nature of this interaction in more detail by probing the local CO geometry and the CO–CO interaction via E versus $k_{\|}$ dispersion measurements. The results of such a study are presented in this paper. We show that (i) the measured band dispersions of the coadsorbate are compatible with the structure model (see fig. 1) proposed for the (2 × 1) LEED pattern, and a comparison of the measured bandwidths with those of other pure CO adsorbates indicates that at least the 4σ wave function of the adsorbed CO in the coadsorbate is very similar to the 4σ wave function in pure CO adsorbates, (ii) the distortion of the CO wave function in the oxygen–CO coadsorbate is considerably less pronounced as compared to alkali–CO coadsorbates [23], (iii) the shift of CO binding energies in the coadsorbate is probably due to CO–CO interaction rather than CO–O interaction, and (iv) a slight tilt of the CO molecular axis with respect to the Pd(111) surface normal is compatible with light polarization dependent measurements, and with the angular dependence of the 4σ shape resonance intensities.

2. Theoretical details and results

We have carried out tight-binding calculations using semi-empirical CNDO-type wave functions and assuming nearest neighbour interactions to determine the band structure of the CO + O coadsorbate overlayer. Details of this theoretical method have been given elsewhere [24,25]. Fig. 1a shows the CO + O (2 × 1) structure model of the coadsorbate. Because of the hexagonal symmetry of the substrate layer there are three possible orientations for the

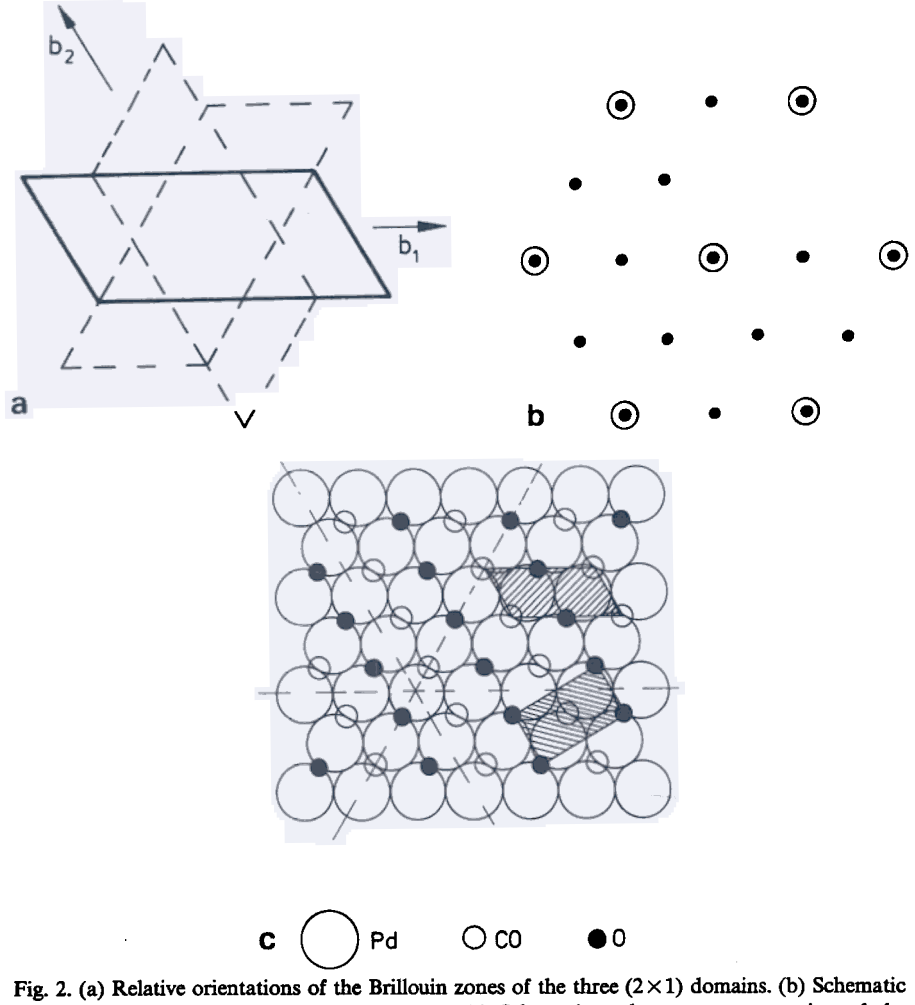

Fig. 2. (a) Relative orientations of the Brillouin zones of the three (2×1) domains. (b) Schematic LEED pattern of the CO+O (2×1) structure. (c) Schematic real space representation of the CO+O (2×1) structure. Two possible elementary cells are given.

coadsorbate domains as indicated in fig. 1b. The resulting Brillouin zones and the schematic LEED pattern are shown in figs. 2a and 2b, respectively. If we consider the isolated coadsorbate overlayer, neglecting the interaction with the substrate, we do not have to use the hexagonal unit cell shown in fig. 2c, but can rather use the orthogonal unit cell as indicated in the same figure. Our calculations have been performed using the orthogonal unit cell. The neglect of the interaction of the overlayer with the substrate, certainly, is a severe approximation. However, we have shown for pure CO overlayers, that the use

of renormalized CO wave functions yields rather satisfactory results for band dispersions [24,25]. One has to remember that coupling between the surface and CO is relatively weak as compared to the oxygen metal interaction. We have therefore tried to take the latter interaction into account by performing a cluster calculation on a Pd_2O cluster using our semi-empirical method [26], and to use the resulting relative ordering and occupancy of the oxygen levels as input for our band calculations.

In order to discuss in a systematic fashion the band structure of the coadsorbate we start with an analysis of the band structure of the CO sublattice. Fig. 3a shows the calculated tight-binding band structure of the isolated CO sublattice in one of the three domains, where the geometric structure has been chosen according to the CO + O (2 × 1) coadsorbate. The bands are labelled according to their orbital parentage, as well as to the translational symmetry of the space group of the coadsorbate (P_{2mm}). The band at highest binding energy is the 4σ derived band. Its dispersion can be easily understood on the basis of the schematic wave function representations shown in fig. 4a. The phases of an s- or σ-type wave function at three points of high symmetry in the surface Brillouin zone are given. At Γ the basis functions are all in phase. Therefore the two-dimensional wave function is strongly bonding, which leads to a stabilization on the binding energy scale relative to the laterally non-interacting CO wave function. The orbital energies of a single CO molecule are given as dashed lines. As we move towards the zone boundary the phases change. At X the wave functions perpendicular to the closed packed rows are out of phase, at Y the wave functions along these rows are out of phase. This leads to an increase of antibonding character in the wave function and therefore to a destabilization of the band on the binding energy scale. Therefore, at Γ the 4σ band energy is minimal, and the maxima at the zone boundary depend on the k-direction, because the antibonding character depends on the magnitude of the interaction between nearest neighbours. Clearly, the interaction is stronger along the close packed rows than perpendicular to the rows.

The 5σ band behaves very similar to the 4σ band if we take the altered interaction parameters for CO–CO interaction into account. The CO 1π bands, on the other hand, exhibit a quite different behaviour. To begin with, one has to remember that the two CO 1π components are no longer degenerate within the overlayer symmetry, because the two perpendicular, Σ and Δ directions are not equivalent. Next, consider the $1\pi_y$ component as an example. At Γ the wave functions are antibonding along the closed packed rows (see fig. 4b), while they are bonding perpendicular to this direction. Since the interaction along the rows is considerably stronger than perpendicular to the rows the overall character of the wave function is antibonding, and it is, consequently, strongly destabilized on the binding energy scale. At X the wave function becomes antibonding in both directions (fig. 4b), but, the additional

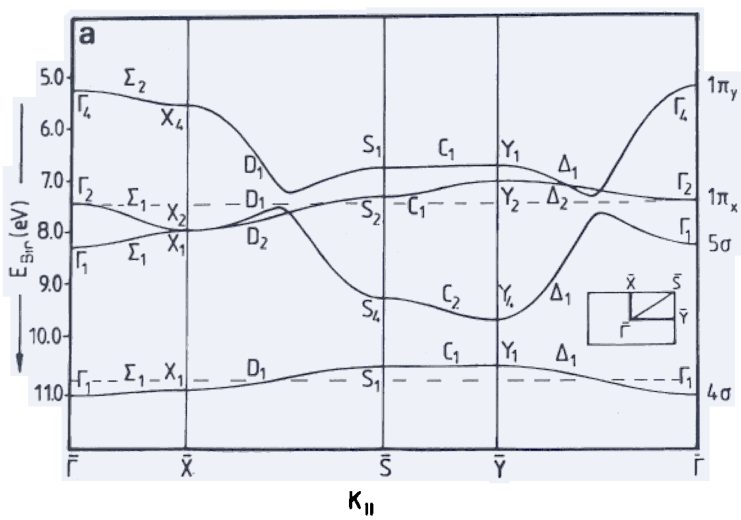

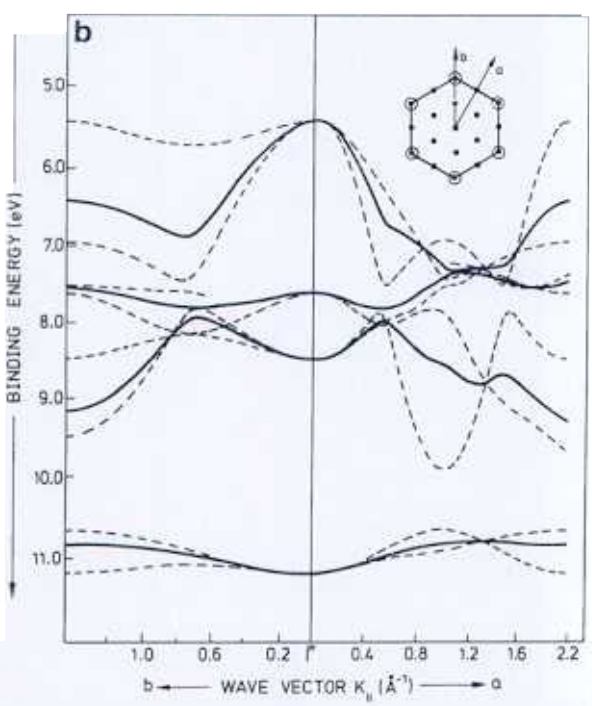

Fig. 3. (a) Calculated two-dimensional band structure of the CO sublattice (one domain) using the geometry of the CO+O(2×1)/Pd(111) structure. (b) Averaged band structure (full lines) along the measured directions "a" and "b" (see fig. 8). The bands in the superimposed domains are shown individually as dashed lines.

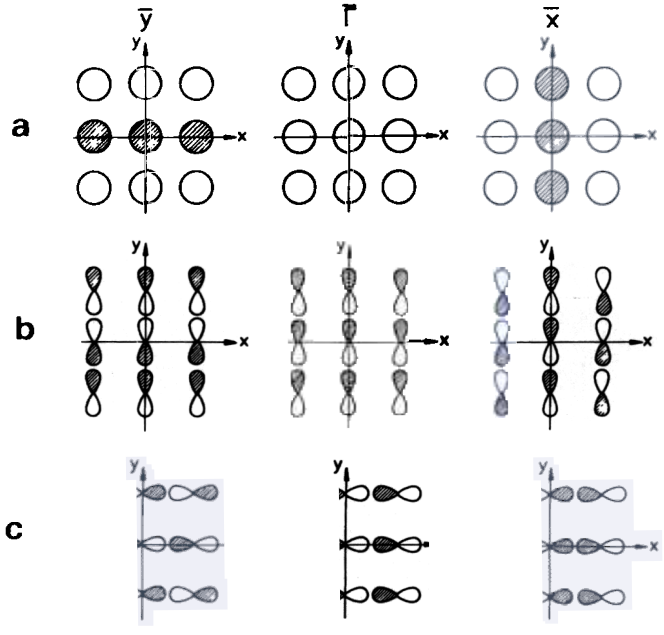

Fig. 4. Schematic representations of the two-dimensional wave functions at three high symmetry points in the SBZ as indicated. (a) s- (or σ-) type wave functions, (b) p_y- (or π_y-) type wave functions, (c) p_x- (or π_x-) type wave functions.

antibonding interaction in x-direction has π-character. Note, that this, however, induces larger σ-bonding character along the x/y diagonal, so that the overall wave function at X is slightly stabilized with respect to Γ. Very little dispersion of this band is the consequence. In contrast, at Y the wave function is strongly stabilized with respect to Γ, because there is a strong increase in bonding character, as can be easily seen by inspection of fig. 4b. This band shows the strongest dispersion of all the bands. It must be expected from the above analysis that the dispersion of the $1\pi_x$ derived bands (fig. 4c) is smaller than that of the $1\pi_y$ derived bands. Fig. 3a corroborates this assumption.

The last step in the discussion of the CO sublattice band structure is to consider $5\sigma/1\pi$ hybridization. This occurs because the two band systems are situated in the same energy region which is typical for the adsorbed molecule, due to the relative stabilization of the 5σ orbital via bonding to the surface. A σ/π = hybridization is not expected if the 5σ–1π energy separation were still the same as in the free molecule. Fig. 3a shows that hybridization occurs between bands of equal symmetry, and its strength depends on the 5σ–1π overlap. One of the consequences of the $5\sigma/1\pi$ hybridization is a maximum of the 5σ derived band within the Brillouin zone along the Δ direction (Γ to Y).

The calculation in fig. 3a has been performed for one domain. However, experimentally it is impossible to measure the dispersion in one zone separately, but one rather averages over the dispersions in three domains. We have to try to simulate this situation computationally. We do this simply, here, by superimposing the three dispersions calculated while we fix their orientation with respect to the substrate, and thus fix the azimuthal direction chosen experimentally. Then we calculate the average band position by assuming that the intensities of the three composing bands are equally weighted. The latter point may be a rather severe approximation, but it is the simplest (and savest) one to assume without explicit intensity calculations. The result of such a procedure is shown in fig. 3b for the experimentally studied directions "a" and "b" (see discussion).

To complete the discussion of the band structure of the CO + O coadsorbate we try to include the oxygen sublattice. The oxygen basis functions have been chosen by performing a cluster calculation on a Pd_2O cluster, then cut off the oxygen from the metal, and, finally, renormalize the wave function. The oxygen atom is only slightly negatively charged (approximately 6.1 e). One oxygen orbital, which is situated at high binding energy below 20 eV, has mainly O 2s character, and is not further discussed in the present study. In addition there are the O 2p orbitals, which are not degenerate as in the free atom, but rather split according to the specific interaction with the metal substrate. The O $2p_z$ and O $2p_x$ orbitals are stabilized to higher binding energies, while the O $2p_y$ orbital is located at lower binding energy. With respect to the CO induced $5\sigma/1\pi$ levels the O $2p_z/2p_x$ levels are at about 2 eV lower binding energy and are split by about 1 eV. This places them at 6.5 eV (O $2p_x$) and 5.5 eV (O $2p_z$) binding energy, approximately, which is just below the metal d/s bands reaching down to 5 eV binding energy. The O $2p_y$ orbital is situated within the region of the metal levels, and will therefore experience strong mixing with the metal levels. A simplified calculation, as presented here, can only be justified for those levels well separated from the metal levels. While we feel it is fully justified for the CO induced levels, we think that the calculated oxygen induced band structure is less reliable. A more complete calculation has to take the substrate band structure into account.

A band structure calculation for the oxygen sublattice is shown in fig. 5 as the bold lines. The two bands derived from O $2p_z$ and O $2p_x$ orbitals at high binding energies behave like the s-type, and $1\pi_x$-type wave functions. Their dispersion is relatively weak and can be explained using the schematic wave function representations in figs. 4a and 4c. The oxygen derived band for which we expect a pronounced dispersion, i.e., the O $2p_y$ band (compare the schematic wave function in fig. 4b) is not shown, and is situated within the region of metal states. The band structure of the CO sublattice shown in fig. 3a, and discussed above, has been added as dashed lines. The symmetry labelling shows that hybridization between CO and O sublattice band structures have

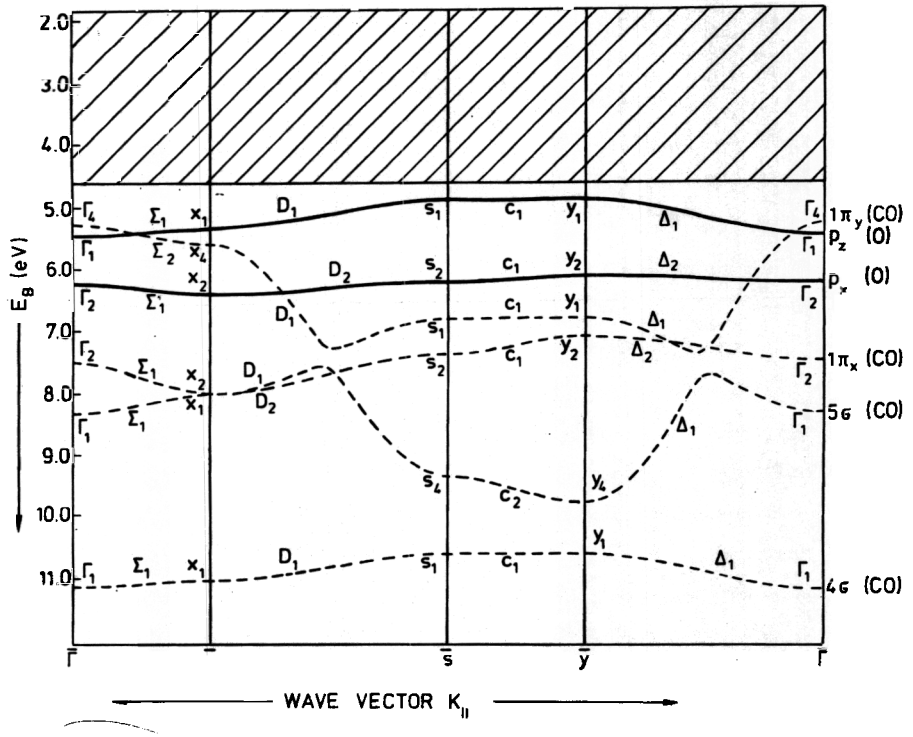

Fig. 5. Complete calculated two-dimensional band structure of the CO+O(2×1)/Pd(111) adsorbate. CO induced bands are shown as dashed lines, oxygen induced bands as full lines. The region of Pd induced features is shown as a hatched area.

not to be expected. We find a strong overlap only between the O $2p_x$ and the CO $1\pi_x$ orbitals. Since these bands are energetically separated we do not find strong hybridization effects. However, the CO 4σ wave function remains more or less unchanged. Thus, if there is any influence we would expect it to be noticeable only for the $5\sigma/1\pi$ bands.

3. Experimental details and results

The experiments were performed in a magnetically shielded ultrahigh vacuum system (VG, ADES400) containing facilities for low energy electron diffraction (LEED), Auger electron spectroscopy (AES), residual gas analysis with a quadrupole mass spectrometer, and angle resolved photoelectron spectroscopy (ARUPS). The electron analyser is rotatable in two orthogonal planes and electrons are collected within an acceptance angle of $+/-1.5°$. Excitation of photoelectrons was achieved by synchrotron radiation from the

exit slit of a toroidal grating monochromator (TGM) attached to the storage ring BESSY in Berlin. The resolution was typically 100 meV. The base pressure in the system was below 10^{-8} Pa.

The Pd(111) crystal was spot-welded between two tungsten wires which were spot-welded to two tungsten rods mounted on a sample manipulator. With liquid nitrogen the crystal could be cooled to 80 K. Heating was possible either by electron impact onto the reverse side of the crystal or by passing a current through the sample. The surface was cleaned by argon ion bombardment. After annealing the cleanliness was checked with AES, and surface order and geometry were established by LEED. For work function measurements using the high energy cut-off of the photoemission spectrum the crystal was biased by -10 eV.

To prepare the various adsorbate overlayers the following procedures have been adopted. They were similar to those described by Conrad et al. [9,14]. For a pure CO overlayer with a sharp $(\sqrt{3} \times \sqrt{3})$R30° LEED pattern the clean crystal with a work function of 6.08 eV was dosed with 1.1 L (langmuir) of CO (Linde AG) at 80 K. This leads to a work function increase to 6.40 eV. A dose of 3 L molecular oxygen at 200 K gave rise to a well ordered p(2 × 2) LEED pattern and increased the work function to 6.19 eV. If a slightly diffuse p(2 × 2) oxygen LEED pattern which was formed by exposing a clean crystal with 2 L oxygen at 200 K, is exposed to CO at the same temperature, the p(2 × 2) spots become sharper, and at the same time $(\sqrt{3} \times \sqrt{3})$R30° spots appear. Further exposure up to 1.4 L of CO at 200 K leads initially to the disappearance of the p(2 × 2) spots, and instead only $(\sqrt{3} \times \sqrt{3})$R30° spots are observed. Subsequently the spots of a (2 × 1) structure appear in addition to the remaining reflexes of the $(\sqrt{3} \times \sqrt{3})$R30° structure. The work function of the final coadsorbate system is 6.31 eV. The photoelectron spectra taken on the various systems under different experimental conditions are collected in figs. 6–11.

4. Discussion

Fig. 6 shows a set of series of spectra for a clean, CO$(\sqrt{3} \times \sqrt{3})$R30° covered, O p(2 × 2) and CO$(\sqrt{3} \times \sqrt{3})$R30° (in domains) covered, and a CO + O (2 × 1) co-adsorbed covered Pd(111) surface taken with z-polarized light in normal emission (fig. 6a), at 40° off-normal emission (fig. 6b), and with s-polarized light in normal emission (fig. 6c). Strong polarization dependent effects are observed especially in the region of the Pd induced d and s bands, which are observed in accord with previous studies down to about 4–5 eV binding energy below the Fermi edge [4,9,27,28]. This is observed in all spectra, and in particular for the clean Pd(111) surface. It can be explained via symmetry considerations on the initial and final metal states involved in the

photoemission process [28]. In the present work we shall not consider this aspect in any further detail. In contrast, we want to consider the adsorbate induced photoemission peaks. Above the spectra of the clean surface in figs. 6a–6c spectra taken on a pure CO adsorbate exhibiting a $(\sqrt{3} \times \sqrt{3})R30°$ LEED pattern are shown. At 7.9 and 10.65 eV the characteristic CO induced $5\sigma/1\pi$- and 4σ-peaks are observed. These binding energies as well as the observed polarization dependence are very similar to CO adsorbates on other transition metal surfaces. If we expose the Pd(111) surface first to molecular oxygen so that a $p(2 \times 2)$ LEED pattern forms and subsequently to a low CO dosis, where the CO is adsorbed in separate islands of $(\sqrt{3} \times \sqrt{3})R30°$ symmetry, then we record spectra shown above the pure CO adsorbate spectra. The CO induced peaks are rather weak but an analysis shows that the

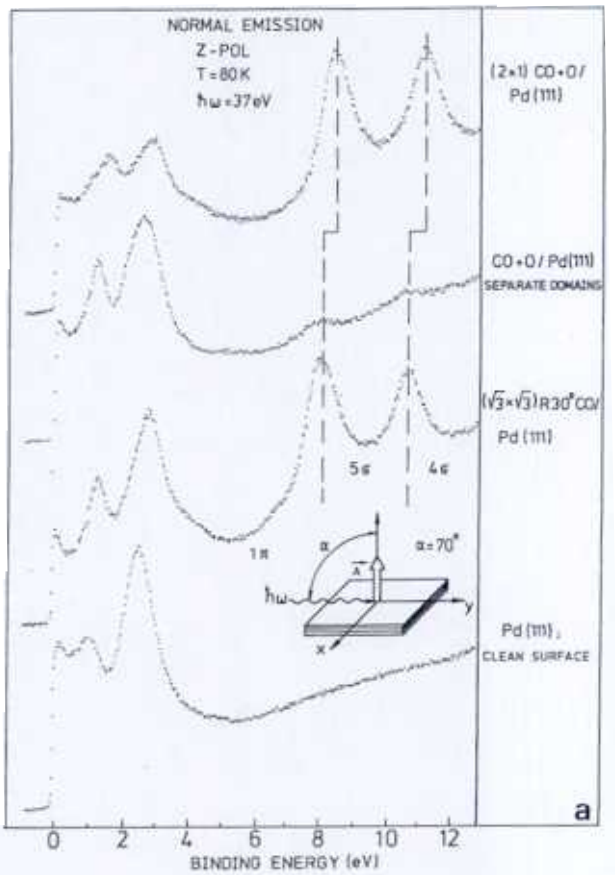

Fig. 6a. Photoelectron spectra of the clean and adsorbate covered Pd(111) surface at 80 K. z-polarization and normal emission.

binding energies as well as the polarization dependence of the intensities is identical to the pure CO adsorbate corroborating the idea that adsorption takes place in separate islands. Interestingly, and different to other oxygen adsorbates, the usually observed intense oxygen induced peaks at about 6 eV binding energy are very weak in the present system. Only in the difference spectra where we have used spectra taken with lower photon energy, i.e. $h\nu = 29$ eV, outside the resonance region of the CO σ induced levels, shown in fig. 7, do we find a clear indication (arrow) of the oxygen induced peaks. However, rather pronounced changes in the region of the metal states are observed. There exists an extended literature on the absence of oxygen induced peaks on 4d and 5d transition metals as compared to 3d transition metals [29,30]. We suggest here, that it is the rather strong mixing of the

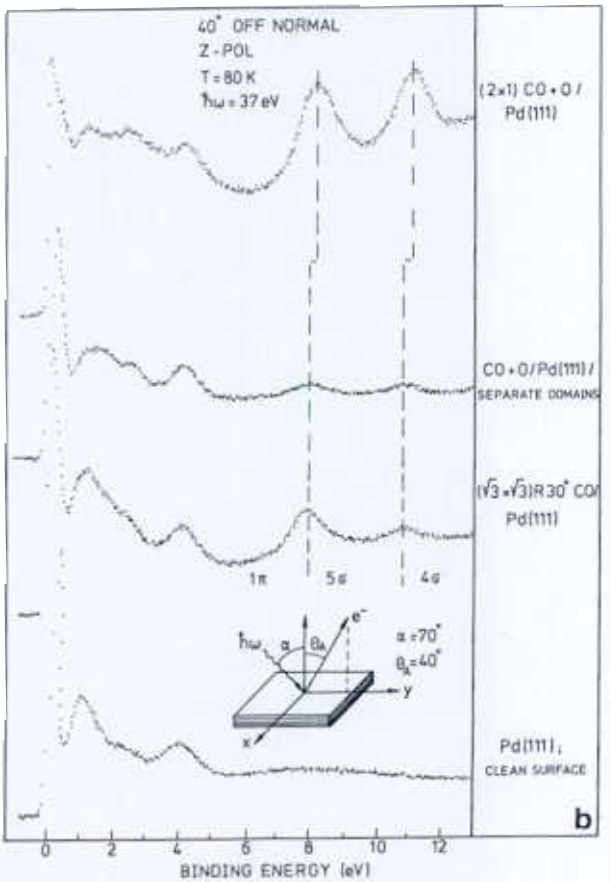

Fig. 6b. Photoelectron spectra of the clean and adsorbate covered Pd(111) surface at 80 K. z-polarization and 40 °-off-normal emission.

oxygen with the low lying metal levels which causes this attenuation of the oxygen induced levels. Later in this paper, when we compare theoretical and experimental results, shall we reconsider this problem in slightly more detail.

Upon dosing the coadsorbate, where CO and oxygen are adsorbed in separate domains, with more CO from the gas phase we compress the coadsorbate structure until a (2×1) LEED pattern can be observed. The topmost curves in figs. 6a–6c are taken on this structure. The important observation is the strong change in the spectral features: In addition to the expected increase in intensity of the CO induced peaks which is due to the higher CO coverage in the (2×1) phase a pronounced shift of the CO peaks, i.e. 0.4 eV for the $5\sigma/1\pi$ peak, and 0.32 eV for the 4σ peak, to higher binding energies, and the metal state emission changes. Furthermore, the polarization

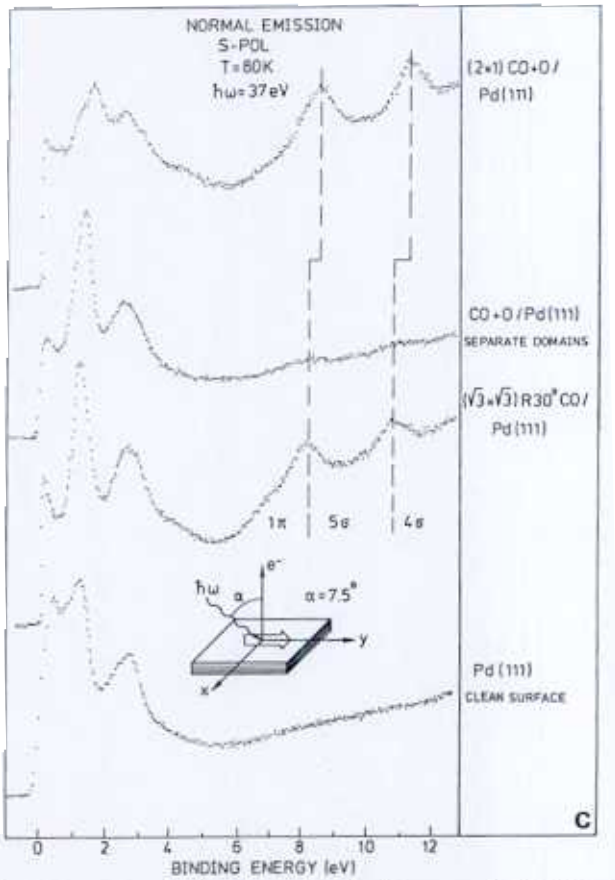

Fig. 6c. Photoelectron spectra of the clean and adsorbate covered Pd(111) surface at 80 K. s-polarization and normal emission.

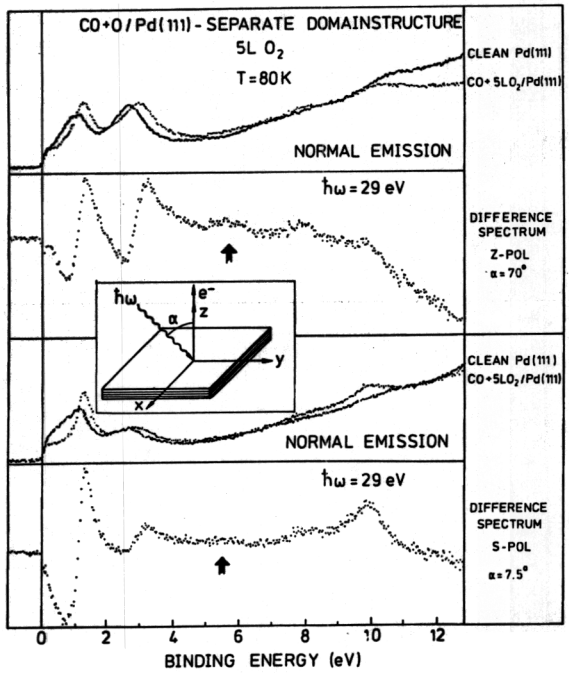

Fig. 7. Difference spectra between oxygen (+CO) covered Pd(111) and a clean Pd(111) surface at 29 eV photon energy (upper panel: z-polarization and normal emission, lower panel: s-polarization and normal emission).

dependence of the intensities of the CO induced peaks is different in the coadsorbed (2×1) phase as compared to the pure CO adsorbate. The relatively more intense 4σ peak for off-normal photoemission and the attenuation of the possibly 1π induced peak found at 7 eV for s-polarized light in normal emission are two significant differences. The most likely explanation for this observation is to assume some kind of lowering of the symmetry of the adsorbate complex, because we know from previous experience on pure CO adsorbates that symmetry dictates to a large extent the angular intensity distributions of CO induced peaks [31]. There are two main possibilities how such a symmetry lowering could be achieved. Firstly, the interaction between adsorbed CO and oxygen could lead to specific directed orbital couplings such that the axial symmetry, and therefore the wave functions of the CO molecules are strongly distorted. Secondly, a deviation from the canonical adsorption geometry, namely a tilt of the CO molecular axis from the usually assumed perpendicular bonding configuration would lead to a symmetry reduction. Of course, both effects could be operative simultaneously. Obviously, it is very hard to separate the effects. We adopt the following procedure, to try to

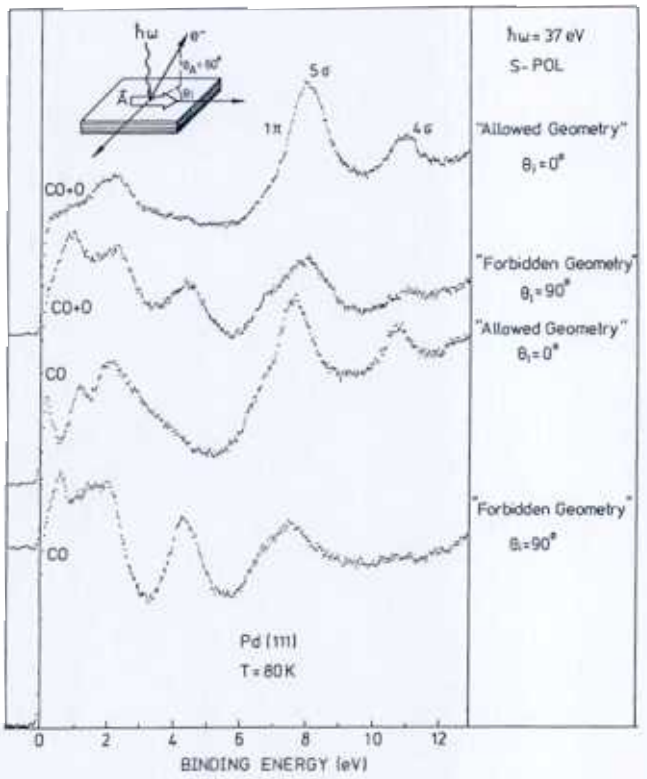

Fig. 8. Photoelectron spectra of a CO($\sqrt{3} \times \sqrt{3}$)R30°/Pd(111) structure and a CO+O (2×1)/Pd(111) structure in "allowed" and "forbidden" geometry.

disentangle the contributions: Experiments within the so-called allowed and forbidden geometries as well as the analysis of the angular dependence of the σ-shape resonances allow conclusions about the local CO geometry as has been shown in the past [31]. Recording the E versus $k_{\|}$ dispersions within the CO adsorbate overlayer, on the other hand, and the comparison with dispersions measured for pure CO adsorbates [23–26], should reveal whether strong changes of the CO wave functions in the coadsorbate occur. In the following we present the results of such experiments.

First, we shall consider geometry sensitive experiments. Fig. 8 shows spectra of the pure CO ($\sqrt{3} \times \sqrt{3}$)R30° adsorbate, and the CO + O (2 × 1) coadsorbate taken in the allowed and forbidden geometries. Here the polarization of the electric field vector is oriented parallel to one of the three mirror planes of the Pd(111) surface. In the allowed geometry the emission is detected in the plane of incidence, which means that initial states which are symmetric to the mirror plane, i.e., 5σ, 4σ, and the even component of the 1π wave

function, are observed, while in the forbidden geometry only the odd component of the 1π wave function has a finite emission probability, provided the CO molecular axis is oriented perpendicular to the surface plane. Clearly, the two spectra in fig. 8 taken on the pure CO adsorbate show exactly this behaviour. For example, the 4σ emission disappears completely upon changing from the allowed to the forbidden geometry. Note at this point, that concommitantly with the intensity changes in the CO induced levels symmetry selection rules also cause pronounced variations of the intensities of the metal emissions. The CO induced peak shown in the forbidden geometry verifies that the shoulder in the $5\sigma/1\pi$ peak at low binding energy has mostly 1π-character.

In the coadsorbate spectra shown in fig. 8 the attenuation of the 4σ emission is still considerably pronounced, but less complete than in the case of the pure CO adsorbate. This result indicates a, probably, slight change in the geometry of the adsorbed CO. However, before we jump to this conclusion it is necessary to take into account alternative explanations. For example, we have used one out of the three Pd(111) mirror planes to define the direction of the electric field vector, and therefore to define the allowed and forbidden geometry. Furthermore, since the three CO + O domains (fig. 1b) are pinned to the three Pd(111) mirror planes, if the proposed structure model is correct, then the allowed and forbidden conditions are only fulfilled for one out of the three CO + O domains. However, in general it is assumed [31] that the substrate does not strongly interact with 4σ electrons of adsorbed CO, and that therefore the global symmetry, including the substrate, is less important than the local CO symmetry. Also, if indeed the 4σ intensity were due to the existence of three domains, its relative intensity with respect to the $5\sigma/1\pi$ peak should be larger. The apparent attenuation of the 1π component of the $5\sigma/1\pi$ peak in the coadsorbate with respect to the pure CO adsorbate, noted in connection with the discussion of fig. 6, is not seen in the forbidden spectrum. The 1π peak is shifted to higher binding energy by an amount comparable to the 5σ shift.

A tool which has been used frequently in the past to investigate molecular orientation, is to study the angular dependence of the σ-shape resonance [31]. Again it is important to study the same effect for the pure CO adsorbate and the CO + O adsorbate in parallel. The results are presented in fig. 9 for pure CO adsorption, and in fig. 10 for CO + O coadsorption. Figs. 9a and 10a show as examples photon energy dependent series in normal emission excited with z-polarized light for the pure CO adsorbate, and the CO + O (2×1) coadsorbate, respectively. Integrating the peak areas for the combined $5\sigma/1\pi$ peak and the 4σ peak choosing different experimental conditions as indicated and plotting them versus photon energy yield figs. 9b and 10b. Care has to be exercised that the Pd Auger transition sweeping through the binding energy region of interest is properly taken into account for photon energies below

30 eV. This can be done almost perfectly for the pure adsorbate, it is more difficult for the coadsorbate. The intensity increase below 30 eV photon energy for the coadsorbate should therefore not be taken as proven. Fig. 9 for the pure CO adsorbate is compatible with the resonance behaviour found for other CO adsorbates on transition metal surfaces. The 4σ resonance clearly peaks for z-polarization and normal emission, and is strongly attenuated for z-polarization and off-normal detection. The 5σ resonance shows a similar behaviour for z-polarization and normal emission. The attenuation for off-normal detection is less pronounced due to scattering effects induced by the substrate [32]. This resonance behaviour is the signature of a CO molecule carbon-end-coordinated and bound perpendicular to the surface plane [32]. It is clear, immediately, by comparison of figs. 9b and 10b that the σ resonances in the coadsorbate are very similar to those in the pure CO adsorbate. The 4σ-resonance is attenuated in off-normal detection directly indicating that the axis of the CO molecule is oriented more or less perpendicular to the surface

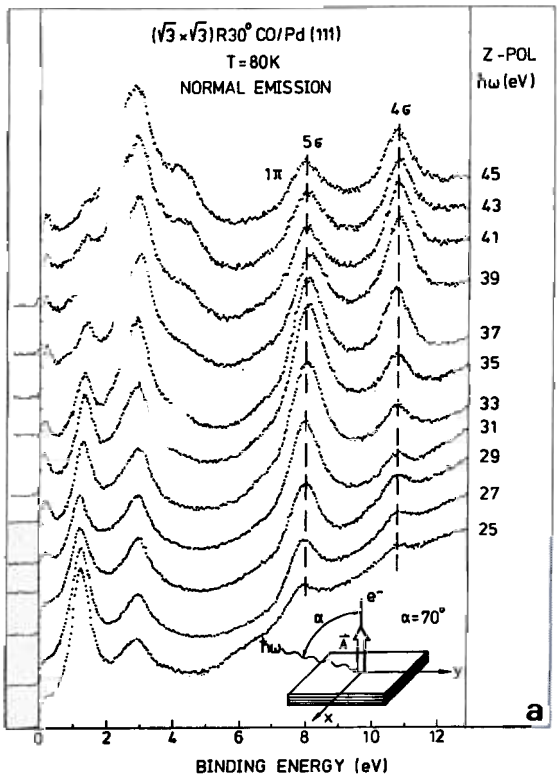

Fig. 9a. Photoelectron spectra of a CO($\sqrt{3} \times \sqrt{3}$)R30°/Pd(111) structure as a function of photon energy using z-polarized light and normal emission detection.

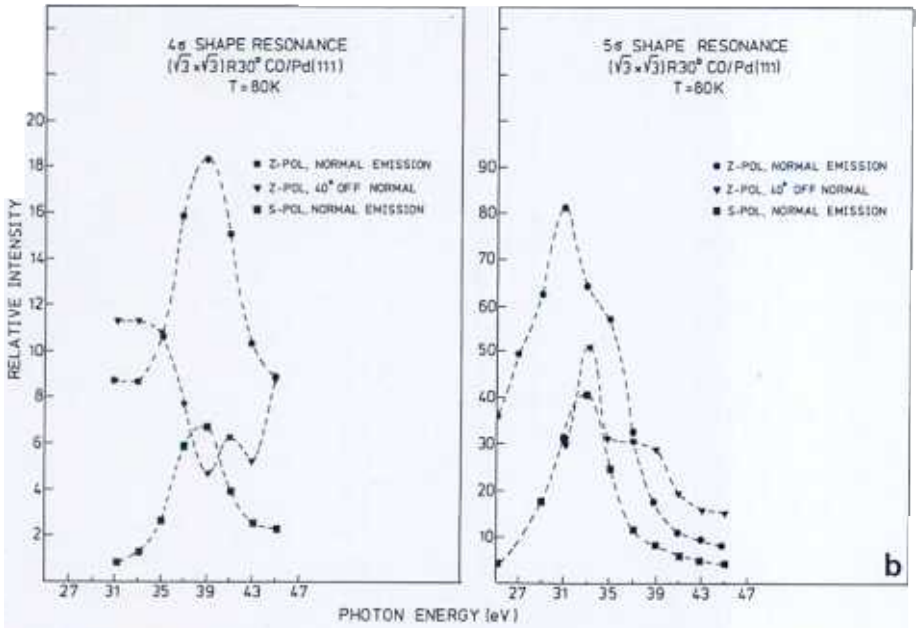

Fig. 9b. Intensities of the CO $5\sigma/1\pi$ and the CO 4σ peaks as a function of photon energy for three different polarization detection geometries. The pass energy of the energy analyser has been changed to 5 eV for those data points taken with z-polarization, normal emission, with respect to the two other detection geometries, where we have chosen $E_{pass} = 7$ eV.

plane also in the coadsorbate. Nevertheless, the measurements in allowed and forbidden geometry, reported above, reveal a slight tilt of the CO molecules. This tilt, however, is probably below a value of 10° and cannot be resolved via the angular dependence of the 4σ shape resonance. To assume a slight tilt of CO in the coadsorbate structure, however, appears reasonable judged by results on a $CO(2 \times 1)P_{2mg}/Pt(110)$ structure [33b]. In the latter system CO is adsorbed along the (110) rows with the same intermolecular separation as in the present case. A slight tilt perpendicular to the (110) rows, giving rise to a (2×1) LEED pattern [34], is a consequence of the close packing. Due to the similarity of the situation it appears reasonable to assume a similar tilt in the case of the coadsorbate structure.

We are now at a point to check and compare the conclusion drawn from the geometry sensitive experiments with wave function sensitive experiments, i.e., the measurement of the E versus $k_{\parallel}$ dispersion. Such experiments reveal, as we shall show below whether the interaction of CO with the oxygen in the coadsorbate breaks the local symmetry and changes the character of the 4σ wave function. Fig. 11 shows two series of spectra where for z-polarized light the polar electron emission angle θ has been varied within two azimuths as

indicated in the figure. Fig. 11a contains the results for the pure CO($\sqrt{3} \times \sqrt{3}$)R30° structure, fig. 11b shows the results for the CO + O (2 × 1) coadsorbate structure. By inspection it is obvious that the dispersion for the coadsorbate is considerably larger as compared to the pure CO adsorbate. Fig. 12 quantifies this statement by showing the measured E versus $k_{\parallel}$ curves for both systems. Table 1 collects some characteristic quantities for the two structures. The 4σ dispersion is very small – hardly observable – in the ($\sqrt{3} \times \sqrt{3}$)R30° structure, i.e., 0.04 eV, and has to be compared to 0.24 eV in the "a" direction and 0.27 eV in the "b" direction of the (2 × 1) structure. This is equivalent to about a factor of seven, and must be caused by the shorter CO–CO distance along the CO rows in the (2 × 1) structure. In the pure CO structure the nearest neighbour distance is 4.71 Å, where each CO is surrounded by six CO molecules. In the (2 × 1) structure the nearest neighbour distance is 2.72 Å but each CO has only two nearest neighbours. The two second nearest neighbours in the (2 × 1) structure are already at a distance of

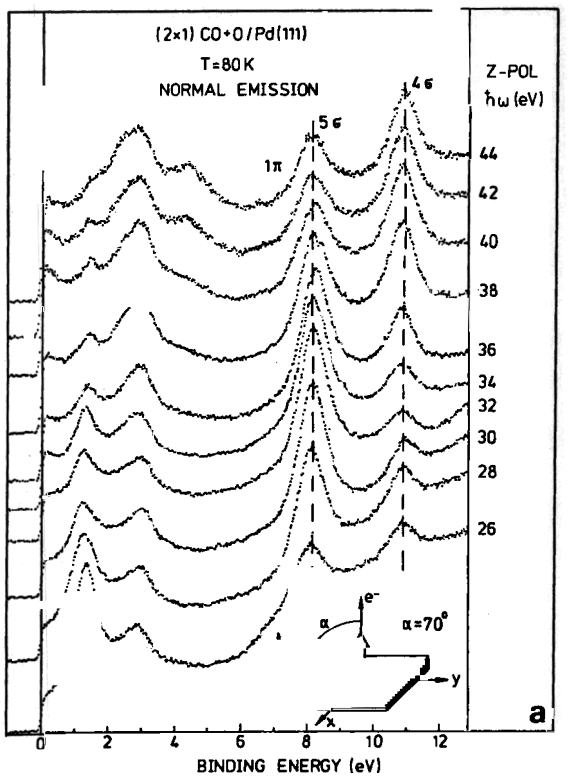

Fig. 10a. Photoelectron spectra of a CO+O(2×1)/Pd(111) structure as a function of photon energy using z-polarized light and normal detection.

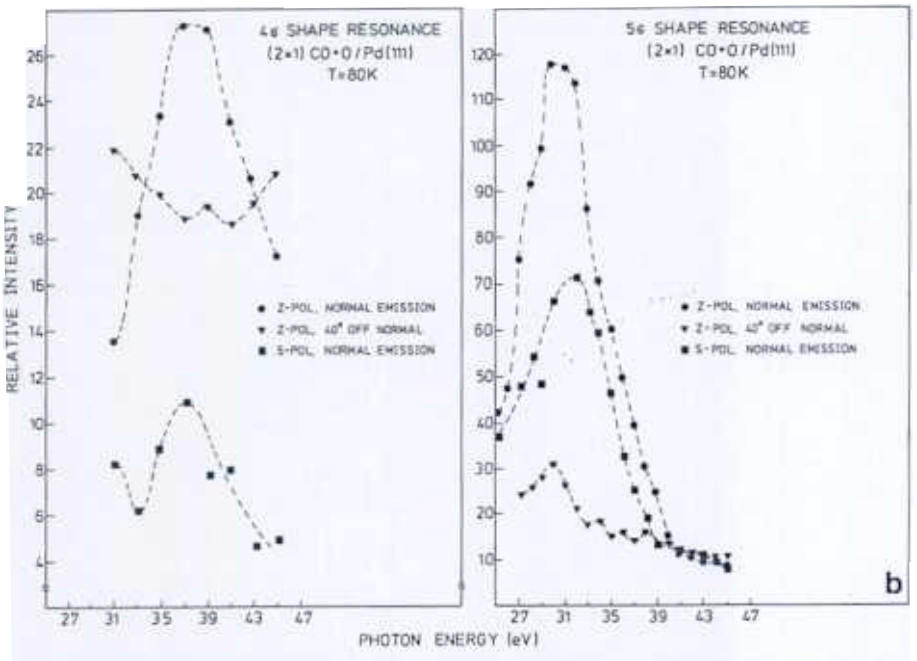

Fig. 10b. Intensities of the CO $5\sigma/1\pi$ and the CO 4σ peaks as a function of photon energy for three different polarization detection geometries. The pass energy of the energy analyser has been 7 eV for all data points.

4.71 Å (equivalent to the $(\sqrt{3} \times \sqrt{3})$ distance). In order to try to understand the dispersions in a more quantitative fashion we compare the measured results to the calculations described in section 3 of the present paper using a procedure successfully applied in the past. It is important to consider that the measured dispersions represent averages over the three domains. The calculation, presented in section 3 (fig. 3b), modelling this average, yields a 4σ dispersion of 0.32 eV in direction "a" and 0.39 eV in direction "b" in reasonable accord with the experimental values of 0.24 and 0.27 eV, respectively. Note, that the calculation has assumed vertical orientation of the molecular axis, and that a slight tilt ($< 10°$) even reduces the bandwidth considerably. No attempt has been made to fit the measured and calculated bandwidths (see however ref. [25]). If we compare the bandwidth determined for the CO + O (2×1) coadsorbate, with 4σ bandwidths of other pure CO overlayers where we have used the hexagonal arrangement as the reference arrangement it is found, as shown in fig. 13, that the present value falls in line with those measured for pure CO overlayers [24,25]. In particular the results are compatible with the dispersion measured by Miranda et al. [35] for the COc(4×2) ‖ Pd(111) structure. For fig. 13 the basic assumption has been

made that the bandwidth is mainly determined by direct through space 4σ-orbital overlap [24]. As a consequence of this assumption we expect a linear relation between the logarithm of the 4σ bandwidth and the intermolecular separation, which is well fulfilled within the experimental scatter. This result suggests that the 4σ wave function is very similar to those of ordinary adsorbed CO, and thus a strong distortion of the 4σ wave function by coadsorbed oxygen can be excluded. The situation here is considerably different from the only other coadsorbate system for which 4σ bandwidths have been determined. Heskett et al. [23] report bandwidths for the ordered CO + K (3 × 3) coadsorbate structure which have been incorporated in fig. 13. Even though in the latter case a definitive structure model has not been proposed, a separation between the adsorbed CO molecules of 4.61 Å has been estimated assuming a CO($\sqrt{3} \times \sqrt{3}$) structure whose free sites are occupied by

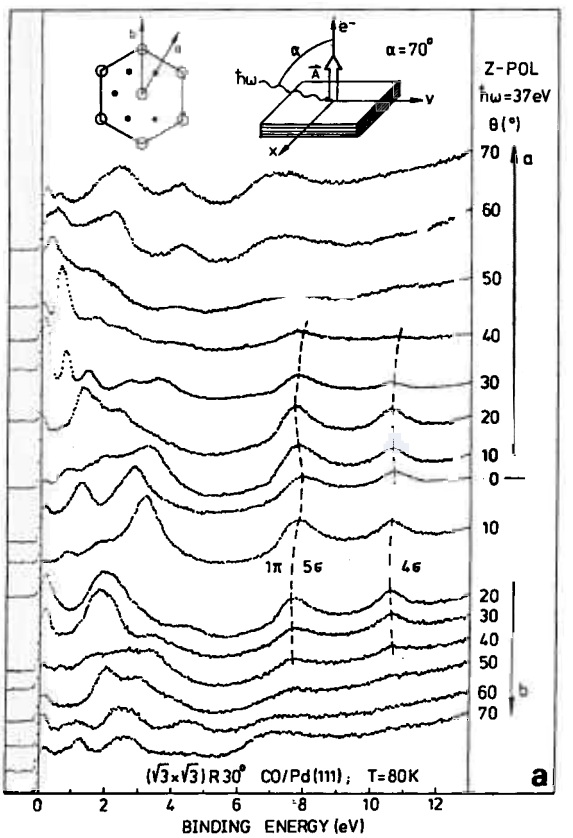

Fig. 11. Series of photoelectron spectra using z-polarized light ($h\nu = 37$ eV) as a function of the polar angle θ. The azimuthal angle is indicated in the schematic LEED pattern (see inset). (a) CO($\sqrt{3} \times \sqrt{3}$)R30°/Pd(111), (b) CO + O (2×1)/Pd(111).

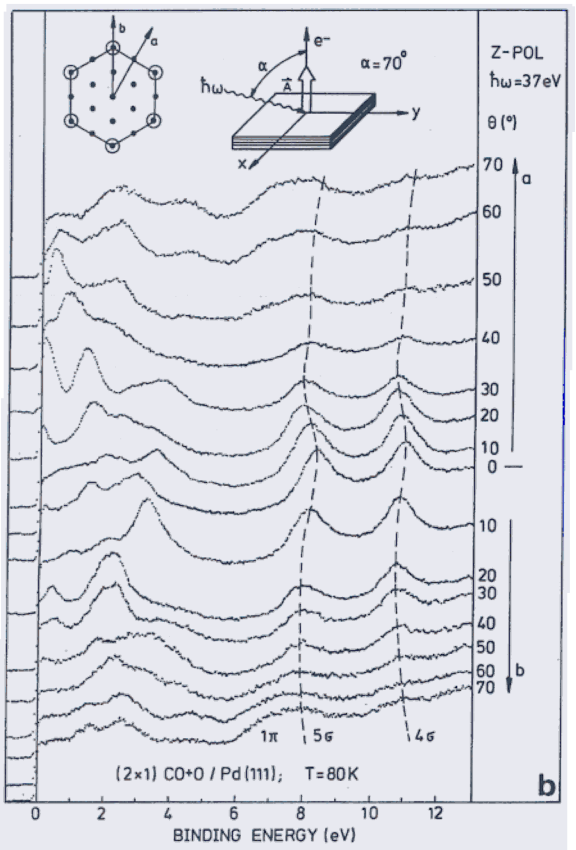

Fig. 11. Continued.

"cationic" K atoms. The measured bandwidths which have been incorporated in fig. 13 show a pronounced deviation from the linear plot which suggests, that the CO 4σ wave function in the case of the CO + K undergoes rehybridization, and is very different from the one in pure CO adsorbates. The fact that coadsorption of K induces changes in the 4σ wave function is known from previous studies, and merely serves in the present case to show that the 4σ dispersion is sensitive to changes of the wave function. We conclude here, that if there are changes in the 4σ wave function for the CO + O (2 × 1) coadsorbate these changes are considerably smaller than for alkali coadsorption. A similar analysis for the 5σ wave function cannot be carried out, because a linear relation in analogy to fig. 13 does not appear to hold [23]. On the other hand this is not surprising since it is very likely that for the 5σ intermolecular interaction several factors, including indirect through metal interactions, in addition to the direct intermolecular overlap are of importance. An indication

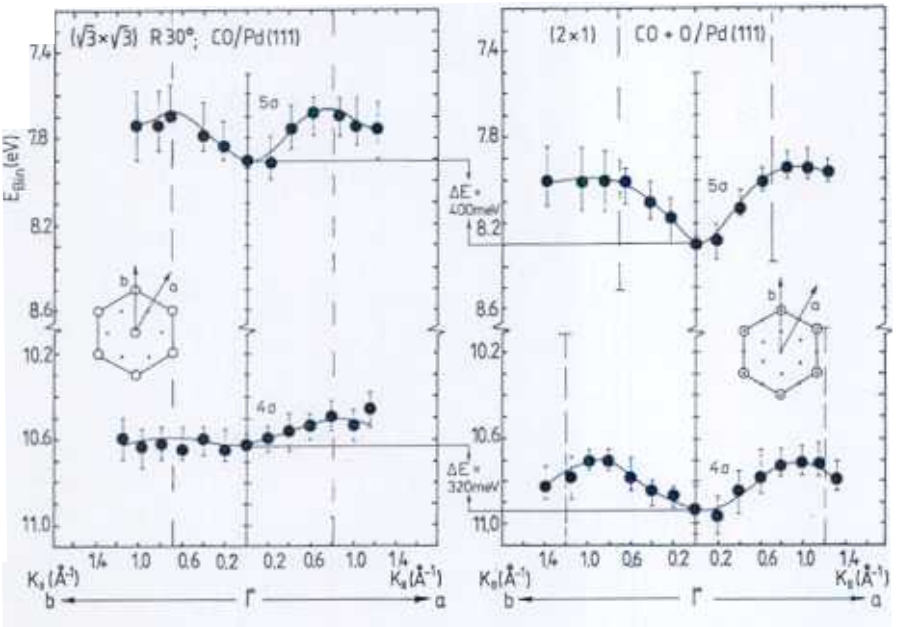

Fig. 12. E versus $k_{\parallel}$ dispersion curves for the CO($\sqrt{3} \times \sqrt{3}$)R30°/Pd(111) structure and the CO + O (2×1)/Pd(111) structure.

can be found in table 1: The 5σ dispersion increases from 0.23 eV (for both "a" and "b" direction) in the ($\sqrt{3} \times \sqrt{3}$)R30° structure to 0.36 eV in direction "a" and 0.30 eV in direction "b" in the CO + O (2 × 1) coadsorbate phase. Compared with the change in the 4σ dispersion this is a relatively small alteration.

To conclude the discussion of the E versus $k_{\parallel}$ dispersions we address the observed turn-around points in the band structure which should correspond to the position of the overlayer Brillouin zone boundary. As is indicated by the dashed vertical lines the condition is well fulfilled for the CO($\sqrt{3} \times \sqrt{3}$)R30°

Table 1
Measured dispersions and turn-around points for the CO($\sqrt{3} \times \sqrt{3}$)R30° and CO + O (2×1) structures

Structure	Orbital	Dispersion "a" (eV)	Dispersion "b" (eV)	Turn-around (Å^{-1})
CO($\sqrt{3} \times \sqrt{3}$)R30°	5σ/1π	0.23	0.23	
	4σ	0.10	0.04	
CO + O (2×1)	5σ/1π	0.36	0.30	
	4σ	0.24	0.27	

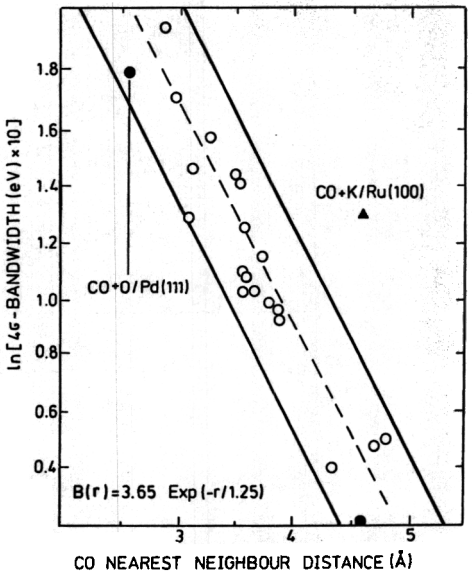

Fig. 13. CO 4σ bandwidths as a function of CO nearest neighbour distances for various substrates. CO bandwidths have been corrected for those structures which are not hexagonal. The bandwidths determined in the present work are shown as filled circles. Data taken from references [23–25,35–41].

structure. However, for the CO + O coadsorbate structure the average over the three domains yields an expected turn-around point slightly larger than the observed one. This, on the other hand, is not unreasonable considering the remaining disorder in the coadsorbate structure as indicated by the relatively diffuse LEED spots. The superimposed Brillouin zones for the three domains as plotted in fig. 2a show, that on the average the first Brillouin zone boundary appears as a "circle" with a radius of 0.8–0.9 Å^{-1} which becomes even more accentuated if the three domain system is not well ordered. An average turn-around point of 0.8–0.9 Å^{-1} is in very good agreement with the experimental data.

From our analysis we have to conclude that the CO 4σ wave function in the coadsorbate is similar to the 4σ wave function in pure CO. The remaining open question is then, what causes the CO induced features to shift to higher binding energy if not a change in the wave function. A comparison with photoemission results on other CO transition metal systems [24,25,35] reveals that whenever the CO coverage increases the 4σ and the 5σ/1π peaks shift to higher binding energies by several tenth of an eV. For example, in an previous study, Miranda et al. [35] have investigated the CO 4σ dispersion in the dense CO c(4 × 2)/Pd(111) system. They report a binding energy at Γ of 10.95 eV which is very close to the value observed here for the coadsorbate structure.

Their comparison shows that an increase in CO coverage is sufficient to induce the observed shift of the CO levels to higher binding energy. Greuter et al. [24] were led to the conclusion that the lower CO adsorption energy in a phase with high CO density results in a weaker CO metal coupling which in turn leads to a reduction in the metal screening of the molecular hole state. This effect increases the binding energy of the CO induced features and allows a straightforward interpretation of the observed effect. The conclusion from this argument is that the shift observed in the CO induced peaks in the (2×1) structure is a consequence of the close packing of the CO molecules, and not so much a chemical shift induced by oxygen coadsorption.

It is clear so far that the CO wave functions in the coadsorbate do not show any significant variation with respect to pure CO adsorbates. There is only an indication for a slight tilt of the CO molecules. However, as stated above, the oxygen induced levels show pronounced differences to other oxygen transition metal adsorbates which indicate particularly strong oxygen–metal interaction. Fig. 5 shows the calculated band structure for one domain of the complete coadsorbate where CO–O interaction has been taken into account. The full lines are the oxygen induced bands, the dashed lines represent the CO induced bands. The bands caused by the 4σ level have been compared with experiment above after averaging over three domains (fig. 3b). A comparison of the $5\sigma/1\pi$ level induced dispersions is more involved due to σ/π hybridization and O–CO interaction. It is unfortunate that the low cross sections for the oxygen induced features only allow a very limited comparison between theory and experiment. Of course, the simplicity of our calculational scheme limits this comparison as well. As pointed out above the oxygen peaks are only clearly seen in the difference spectra at lower photon energies. They are located around 6 eV binding energy as revealed by the calculation and can be excited by z-polarized light as seen experimentally.

5. Conclusions

In the present study we have studied the electronic structure of an ordered CO + O coadsorbate by means of ARUPS in comparison with a pure CO adsorbate. Experimentally it is found, that:

(i) Upon formation of the coadsorbate the binding energies of the CO induced levels shift to higher binding energies by several tenth of an eV with respect to the pure CO adsorbate.

(ii) Polarization dependent measurements in allowed and forbidden geometry reveal differences between the coadsorbate and the pure adsorbate.

(iii) The angular dependences of the σ-shape resonances in the pure CO adsorbate and the coadsorbate are shown to be the same within experimental error.

(iv) The bandwidth of the 4σ induced CO band in the coadsorbate are by factors larger than in the pure adsorbate. The $5\sigma/1\pi$ bandwidths are much more similar in both systems.

(v) The oxygen induced peaks are very weak.

From these findings we draw the following conclusions:

(i) The CO molecules are oriented with their axis more or less perpendicular to the surface in both the pure CO and the coadsorbate. There may be a slight tilt of the axis below 10° with respect to the surface normal in the coadsorbate.

(ii) The comparison with binding energies in pure CO adsorbates shows that the shift in binding energy observed for the coadsorbate can be fully explained by the higher density of the CO molecules in the coadsorbate as compared with pure CO($\sqrt{3} \times \sqrt{3}$)R30° adsorbate. It is probably not an effect due to oxygen coadsorption.

(iii) The observed strong dispersion of the 4σ band in the coadsorbate can be explained on the basis of a simple tight-binding calculation presented in this paper, and it corroborates the structure model by Conrad et al. [9].

(iv) A comparison of the measured dispersion for the coadsorbate with the dispersion measured for pure CO adsorbates (fig. 13) shows that the 4σ wave function of the CO in the coadsorbate is similar to a 4σ wave function in a pure CO adsorbate.

(v) The situation for oxygen CO coadsorption is with respect to conclusion (iv) different from alkali–CO coadsorbates [23], where a change in the 4σ wave function can be observed via the same procedure.

(vi) The reason for the absence of strong oxygen induced photoemission signals probably is the strong interaction of these levels with the substrate wave functions.

The general conclusion with respect to CO_2 formation, which has been the motivation for this study can be summarized as follows: There is no very strong distortion fo the CO wave functions due the coadsorbed oxygen. Therefore, the individual adsorbed species retain their properties, i.e., there is no sign of any CO_2 preformation in the coadsorbate. Then the question arises, why is this coadsorbate structure so reactive with respect to CO_2 formation [1]? The reason is that the CO molecules are activated by the strong intermolecular repulsion. As a consequence of this repulsion the contact between metal surface and CO is weakened, so that upon heating of the substrate the electronic rearrangement connected with the disruption of the CO metal bond is initiated and a very reactive CO species is formed, which, instead of desorbing binds the oxygen in very close proximity. The OC–O bond formation yields the sufficient amount of energy to overcome the oxygen–metal bond. It is known from independent studies that CO_2 itself does not chemically bind to Pd(111). Also, the coadsorbate is so crowded that the neighbouring adsorbed species push the nascent CO_2 molecules off the surface, and

cause, as has been discussed by Matsushima et al. [2], the strong forward collimation of the desorbing molecules. Summarizing, it is the "interdiffusion" of CO and oxygen, and particular the compression of the CO–CO intermolecular distance that leads to the activation of the system and finally to the formation of CO_2.

Acknowledgements

We are grateful to the "Deutsche Forschungsgemeinschaft", and "Fonds der Chemischen Industrie" for financial support. This work has been supported in part by "Bundesministerium für Forschung und Technologie". E.W.P. thanks the Alexander-von-Humboldt Stiftung for a fellowship (Humboldt-Award). We are grateful to Dr. D. Heskett for providing the details of his measurements in ref. [23].

References

[1] T. Engel and G. Ertl, Advan. Catalysis 28 (1979) 1.
[2] T. Matsushima and H. Asada, J. Chem. Phys. 85 (1986) 1658.
[3] V. Matolin, S. Channakhone and E. Gillet, Surface Sci. 164 (1985) 209.
[4] P.V. Kamath and C.N.R. Rao, J. Phys. Chem. 88 (1984) 464.
[5] J.S. Close and J.M. White, J. Catalysis 36 (1975) 185.
[6] E.M. Stuve, R.J. Madix and C.R. Brundle, Surface Sci. 146 (1985) 155.
[7] N.K. Ray and A.B. Anderson, Surface Sci. 119 (1982) 35.
[8] J. Goschnik, M. Wolf, M. Grunze, W.N. Unertl, J.H. Block and J. Loboda-Cackovic, Surface Sci. 178 (1986) 831.
[9] H. Conrad, G. Ertl and J. Küppers, Surface Sci. 76 (1978) 323; Z. Naturforsch. 25a (1970) 1906.
[10] T. Engel and G. Ertl, J. Chem. Phys. 69 (1978) 1267.
[11] G. Ertl, Ber. Bunsenges. Phys. Chem. 86 (1982) 425.
[12] T. Engel and G. Ertl, The Chemical Physics of Solid Surfaces and Heterogeneous Catalysis, Vol. 4, Eds. D.A. King and D.P. Woodruff (Elsevier, Amsterdam, 1982) p. 92.
[13] M.P. d'Evelyn and R.J. Madix, Surface Sci. Rept. 3 (1984) 413.
[14] H. Conrad, Dissertation, München (1976).
[15] T. Matsushima, T. Matsui and M. Hashimoto, J. Chem. Phys. (1984) 5151.
[16] T. Matsushima, J. Catalysis 83 (1983) 446.
[17] T. Matsushima, Surface Sci. 127 (1983) 403.
[18] B. Bartos, H.-J. Freund, H. Kuhlenbeck, M. Neumann, H. Lindner and K. Müller, Surface Sci. 179 (1987) 59.
[19] H.-J. Freund, H. Behner, B. Bartos, G. Wedler, H. Kuhlenbeck and M. Neumann, Surface Sci. 180 (1987) 550.
[20] H.-J. Freund and R.P. Messmer, Surface Sci. 172 (1986) 1.
[21] G. Illing, D. Heskett, E.W. Plummer, H.-J. Freund, Th. Lindner, J. Somers, A.M. Bradshaw, U. Buskotte and M. Neumann, to be published.
[22] See for example: F.M. Hoffmann, Surface Sci. Rept. 3 (1983) 107.

[23] D. Heskett, E.W. Plummer, R.A. DePaola, W. Eberhardt, F.M. Hoffmann and H.R. Moser, Surface Sci. 164 (1985) 490.
[24] F. Greuter, D. Heskett, E.W. Plummer and H.-J. Freund, Phys. Rev. B27 (1983) 7117.
[25] H. Kuhlenbeck, M. Neumann and H.-J. Freund, Surface Sci. 173 (1986) 194.
[26] H.-J. Freund, G. Hohlneicher, Theoret. Chim. Acta 51 (1979) 145;
H.-J. Freund, B. Dick and G. Hohlneicher, Theoret. Chim. Acta 57 (1980) 181;
H.-J. Freund, Dissertation, Köln (1978).
[27] F. Greuter, I. Strathy, E.W. Plummer and W. Eberhardt, Phys. Rev. B33 (1986) 736.
[28] F.J. Himpsel and D.E. Eastman, Phys. Rev. B18 (1978) 5236.
[29] K. Wandelt, Surface Sci. Rept. 2 (1982) 1.
[30] D.L. Weissman, M.L. Shek and W.E. Spicer, Surface Sci. 92 (1980) L59.
[31] E.W. Plummer and W. Eberhardt, Advan. Chem. Phys. 49 (1982) 533.
[32] J.W. Davenport, Thesis, University of Pennsylvania (1976); Phys. Rev. Letters 36 (1976) 945.
[33] (a) W. Riedl, Dissertation, München (1985);
(b) D. Rieger, Dissertation, München (1985).
[34] R.M. Lambert, Surface Sci. 49 (1975) 325.
[35] R. Miranda, K. Wandelt, D. Rieger and R.D. Schnell, Surface Sci. 139 (1984) 430.
[36] D. Rieger, R.D. Schnell and W. Steinmann, Surface Sci. 143 (1984) 157.
[37] C.W. Seabury, E.S. Jensen and T.N. Rhodin, Solid State Commun. 37 (1981) 383.
[38] K. Horn, A.M. Bradshaw, K. Hermann and I.P. Batra, Solid State Commun. 31 (1979) 257.
[39] K. Horn, A.M. Bradshaw and K. Jacobi, Surface Sci. 72 (1978) 719.
[40] E.S. Jensen and T.N. Rhodin, Phys. Rev. B27 (1983) 3338.
[41] H.-J. Freund, W. Eberhardt, D. Heskett and E.W. Plummer, Phys. Rev. Letters 50 (1983) 768.